The Nucleus, **46** (4) 2009 : 389-396

The Nucleus
A Quarterly Scientific Journal of Pakistan
Atomic Energy Commission
NCLEAM, ISSN 0029-5698

STUDY OF THE REACTION CROSS SECTION OF 14.0 MeV/u ^{238}U IONS INCIDENT ON ^{51}V TARGET

*G. SHER, M.I. SHAHZAD and MATIULLAH

Physics Division, Directorate of Science, PINSTECH, P.O. Nilore Islamabad, Pakistan

(Received July 14, 2009 and accepted in revised form September 29, 2009)

The reaction cross section of ^{238}U-ions with energy 14.0 MeV /u and incident on a Vanadium target has been investigated using mica track detectors. In this regard, a thin layer (0.56 mg/cm^2) of V was deposited on a clean and smooth sheet of mica in vacuum. This assembly was then irradiated with a fluence of 0.9×10^5 ions/cm^2 normally incident ^{238}U ions at UNILAC accelerator of G.S.I. Darmstadt, Germany. After irradiation, the target layer was removed from the mica detectors which was then etched in HF acid at room temperature for 20 minutes. After counting the tracks under an optical microscope, the elastic track events were separated from two-prong track events using the angular correlation criterion. Using the number of two-prong inelastic and higher multiplicity track events, the total and partial reaction cross-sections were calculated. The experimentally measured total cross section was compared with the cross section calculated using the sharp cut-off model as well as that determined with the quarter-point angle.

Keywords: Heavy ion interaction, Elastic track events, Inelastic multi prong events, Cross-section

1 Introduction

The reaction cross-section is one of the basic parameters required in many areas of science and technology, including applications in medical science, research in atomic and nuclear physics etc. The characteristics of nuclear reaction processes are determined by the entrance channel conditions such as mass of the interacting nuclei, energy of the system and impact parameter. Nuclear reactions are induced when the energy of the projectile exceeds the Coulomb barrier so that the two nuclei can come close enough for nuclear force to act [1, 2]. The study of heavy ion reactions over a wide range of impact parameters, from grazing collision to nearly central impact describes the correlation between observable quantities (e.g. angular distribution, energy and masses of the fragments, etc.). If the energy is a few MeV above the Coulomb barrier then a variety of dissipative processes may take place. In the energy range of 10 MeV/u to 20 MeV/u, with three or more fragments in the exit channel, the reaction mechanism is usually sequential. This implies that in the first reaction step, two excited primary fragments are formed and one or both of them subsequently undergo fission in the second step. In the case of five or more heavy fragments in the exit channel, the reaction process may take place in three or more than three steps [3-5].

Heavy ion reactions have been intensively studied by various research groups in this range of energy and total and partial reaction cross-sections have been reported [7-11]. The statistics of track events having different multiplicities yield the experimental values of total and partial reaction cross-sections. The total reaction cross-sections can also be calculated from the quarter-point angle, which is derived from the angular distribution of elastic data observed in the reaction [11].

The electronic counting systems are very useful for such studies. However, these systems are expensive and can be used only in the on-line mode, which makes them dependent upon the availability of the accelerator facility. To circumvent this problem, solid state nuclear track detectors (SSNTDs) are extensively used in studying heavy ion interactions [12-14]. Energetic charged particles produce permanent damage trails in SSNTDs which are enlarged by chemical etching. The etched tracks are then counted under an optical microscope. Due its excellent spatial resolution of measured fragment trajectories and

* Corresponding author : gsher@pinstech.org.pk

good energy loss resolution, the mica track detector has been successfully used in the study of fragments produced in nuclear collisions at different energies. SSNTD based systems are unique for the measurements of reaction cross-sections of high multiplicities, even with low statistics [15,16]. This article deals with the measurement of reaction cross section of ^{238}U-ions having energies 14.0 MeV /u incident on a Vanadium target using mica track detectors

2. Experimental Procedure

In order to perform this experiment, a 2π target-detector assembly was prepared by vacuum deposition of a thin target layer (0.56 mg/cm^2) of V on a clean and smooth sheet of mica track detector. This assembly was then irradiated with a normally incident beam of mono-energetic ^{238}U ions having energy of 14.0 MeV/u at the UNILAC accelerator of G.S.I. Darmstadt, Germany. The ions fluence was 0.9×10^5 ions/cm^2. Schematic diagram of the irradiation set-up is shown in Fig. 1.

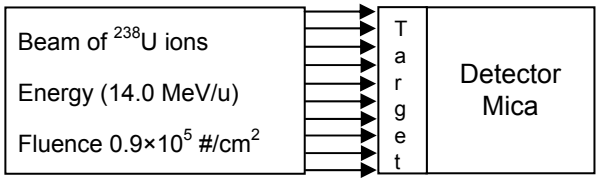

Figure 1. Schematic representation of 2π exposure geometry for the reaction (14.0 MeV/u) ^{238}U + V (mica detector).

The mica (muscovite) detector used had chemical formula $KAl_3\ Si_3O_{10}(OH)_2$, density ~ 2.9g/cm^3 and refractive index = 1.57. The threshold of charge particles detection of mica detector is (Z/β) ~ 400. After exposure the target layer was removed from the surface of the detector using aqua regia (HCl: HNO_3 = 3:1). The thickness of the target layer was determined by weighing the sample before and after the removal of the target material. The detector was then etched in HF at room temperature for 20 minutes and the etched tracks were counted under an optical microscope.

It may be noted here that the tracks produced by the non-interacting incident ions appeared as black dots/spots whereas those which interacted with the target produced two and higher multiplicity tracks having a common vertex inside the target material. Those having azimuthal angle between two consecutive tracks <180º are kinematically complete because all the fragments in the exit channel have been registered, they are called direct (D) track events. In the case, when azimuthal angle between pair of correlated tracks is >180º, one can be certain that at least one fragment balancing the momentum of the fragment emitted in the other direction has not been registered. These incomplete track events are counted in the category of next higher multiplicity for the purpose of determining the cross section and are called indirect (ID) track events. For each projectile and target collision, experimentally observed two and higher multiplicity event are shown in Fig. 2. The fluence of the beam is measured by counting the total number of track openings (dots) caused by both interacted and un-interacted ions in the selected area of the detector. The total number of inelastic track events was used in the measurement of the total cross section. The 2-prong elastic track events are used to calculate the quarter point angle and 3- 4-and 5-prong track events are used to measure the partial cross sections for the respective multiplicity. Table 1 shows the number of binary track events and higher multiplicity track events, the scanned area of detector, the target thickness and fluence of the incident beam which are the required experimental parameters to calculate the reaction cross sections.

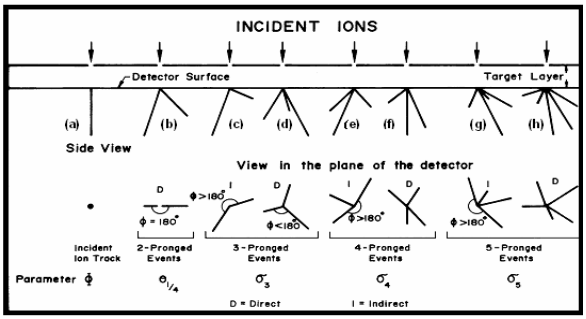

Figure 2. Schematic diagram of the observed etched tracks.

The projected lengths of the tracks have been measured by tracing the image of the tracks using the tracing tube attached with the optical microscope and the length of each traced image was multiplied with the calibration factor of the tube to calculate the projected track length (l_{pi}). The depth of the end point of the tracks has been measured with a linear transducer (Heidenhain depth measuring instrument). The value of the measured depth was multiplied with the refractive index of the etched detector to calculate the actual depth (d_i) of the etched track.

Table 1. Observed binary etched track events, multi-prong track events, scanned area and thickness of the detector and fluence of the incident beam.

2 prong	3 prong	4 prong	5 prong	Total	Scanned Area (cm^2)	Target Thickness (mg/cm^2)	Fluence ($\#/cm^2$)
456	90	25	2	573	13.47 ± 0.03	0.50 ±0.04	$(0.91\pm0.09)\times10^5$

The actual lengths of the tracks (l_i) and the polar angles (θ_i) of the multi-prong track events were calculated from the values of projected lengths (l_{pi}) and depths (d_i) using the following equations.

$$l_i = \sqrt{l_{pi}^2 + d_i^2}\,; \qquad i = 1, 2, 3, \tag{1}$$

$$\text{and } \theta_i = \tan^{-1}\left(\frac{l_{pi}}{d_i}\right) \tag{2}$$

Using the projected lengths for the correlated tracks of every event, the azimuthal angles (φ) were also determined. The two-prong track events have $\varphi = (180 \pm 5)^o$ whilst track events having more than two tracks with φ less than 180^o between the two consecutive tracks were multi-prong track events

2.1 Separation of elastic track events

Binary and higher multiplicity etched tracks were counted. The length and angles of etched track which are required for the calculation of the reaction cross-section were also measured. The elastic track events were selected on the basis of angular correlation between the scattered projectile (i.e. ^{238}U and recoiled target nucleus (^{51}V) after interaction with respect to the incident beam direction.

According to this criterion, for an elastic event the scattering angle of tracks corresponding to the projectile angle θ_1 and target angle θ_2 in the laboratory frame of reference should satisfy the following condition [19].

$$\theta_1 = \tan^{-1}\left[\frac{\sin 2\theta_2}{\frac{A_P}{A_T} - \cos 2\theta_2}\right] \tag{3}$$

where A_P and A_T are the mass numbers of projectile and target atoms. The angles have been calculated from the projected length and depths of the track. The uncertainty in the angles θ_1 and θ_2 were calculated using the following relation.

$$\delta\theta_i = \left[\sqrt{(l_{pi}\,\delta d)^2 + (d_i\,\delta l_p)^2}\,/\,l_i^2\right].180\,/\,\pi \text{ (degree)} \tag{4}$$

where $l_i = \sqrt{l_{pi}^2 + d_i^2}$., i= 1,2 and δl_p and δd are the measurement errors in the projected length and depth of the etched track respectively. For the fixed values of δl_p and δd each prong of an event will have different values of $\delta\theta$. After the application of angular correlation criterion the number of elastic track events are obtained as shown in Fig 3. The small tracks with large scattering angles represent recoiling target nuclei, whereas the scattered projectiles are seen as long tracks with small angles.

The etched tracks with larger values of the scattering angle were observed to have smaller lengths. The tracks are due to the scattering of target atoms whereas those with smaller values of the scattering angles having larger etched length are those produced due to the projectile ion.

3. Results and Analysis

3.1 Reaction cross-section using inelastic data

From the measured values of inelastic track events, scanned area of the detector, target thickness and fluence of the incident beam, the total and partial reaction cross-sections have been determined. The partial reaction cross-section for the different multiplicity of track events is calculated using the following expression:

$$\sigma_n^{exp} = \frac{\chi(n)\,A_T}{N_O\,\Phi\,\rho_t\,a} \tag{5}$$

where $\chi(n)$ is the number of track events of multiplicity 'n' observed within an area 'a', N_o is Avogadro's number, ρ_t is the specific thickness (mg/cm^2) of target having mass number A_T, and Φ is the number of etched track events /cm^2.

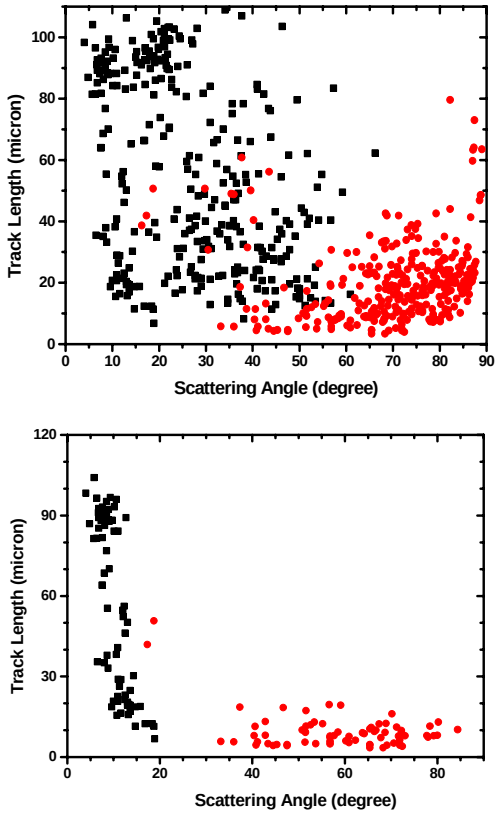

Figure 3. Etched track length as a function of scattering angle for 2-prong track events (each contributes two points; one for the projectile and the other for the target) (a) all track events (b) track events which satisfy the angular correlation.

The total experimental reaction cross-section was determined using the following expression [20]

$$\sigma_{tot}^{exp} = \sigma_2^{exp}(inel) + \sum_{i=3}^{5} \sigma_i^{exp} \qquad (6)$$

where σ_2^{exp} *(inel)* is the two prong inelastic track events cross-section and $\sum_{i=3}^{5} \sigma_i^{exp}$ has been determined using the 3-and 4-prong track events observed in this reaction.

The uncertainties in the measurement of the target thickness ($\delta_{\rho t}$), area (δ_a) and fluence (δ_ϕ) have been estimated to be 8.8%, 2.5% and 8.7 %, respectively. The total uncertainty in the cross sections is given in Table 2.

$$\delta\sigma_n = \frac{\sigma_n}{100}\sqrt{\frac{10000}{\chi(n)} + (\delta_\phi)^2 + (\delta_{\rho t})^2 + (\delta_a)^2} \qquad (7)$$

3.2. *Calculation of the theoretical reaction cross section*

The reaction cross-section σ^{th} was calculated using the sharp cut-off model (Tanabe, et al., 1980).

$$\sigma^{th} = \pi R_{int}^2 \left[1 - \frac{V(R_{int})}{E_{C.M}}\right] \qquad (8)$$

where $E_{C.M.}$ is the energy in the centre-of-mass frame of reference $= \mu E_{lab}$, μ is the reduced mass = $(A_P A_T) / (A_P + A_T)$, $V_{(R_{int})}$ is the Coulomb barrier at the radius of interaction R_{int} of two interacting nuclei having mass number A_P (projectile mass number) and A_T (target mass number).

The Coulomb potential at interaction R_{int} is calculated using the following equation

$$V(R_{int}) = \frac{Z_P Z_T e^2}{R_{int}} \qquad (8a)$$

Z_P and Z_T are the charge of the projectile and target ions, respectively.

The value of the radius of interaction close to the sum of the radii of the interacting nuclei R_{int} is given in terms of the charges Z_P, Z_T and masses A_P, A_T for projectile and target nuclei, respectively.

$$R_{int} = r_o(A_P^{1/3} + A_T^{1/3}) \qquad (9)$$

where r_o is the fundamental radius constant determined to be 1.41± 0.03 fm using the methodology reported [17]. The grazing angular momentum $l_{gr} = l_{max}$ was determined using the following relation

Table 2. The partial cross-sections calculated by using the number of inelastic binary and higher multiplicity track events. The total reaction cross sections determined by inelastic data, total reaction cross section using quarter-point angle and the theoretically calculated total reaction cross section obtained in the reaction (14.0 MeV/u)^{238}U+V, using mica track detectors. The errors incude systematic and statistical uncertainties.

σ2 (barn)	σ3 (barn)	σ4 (barn)	σ5 (barn)	σ_{tot}^{exp} (barn)	σ^{th} (barn)	σ_{el}^{exp} (barn)
2.52±0.5	1.13 ±0.3	0.2± 0.06	0.012±0.02	3.835±0.7	3.871	3.81±0.7

Table 3. The values of the reaction parameters including laboratory energy (E_{Lab}), centre of mass energy ($E_{C.M}$), Sommerfeld parameter(η), the reduced mass (μ), radius of interaction (R_{int}) and Coulomb barrier at radius of interaction V(R_{int})of the reaction (14.0 MeV/u) ^{238}U+V, using mica track detectors.

E_{Lab} (MeV)	$E_{C.M}$ (MeV)	η	μ	$\theta_{1/4}$(C.M) Deg.	R_{int} (fm)	V(R_{int}) (MeV)
3332	588	89.4	42.0	26.30 ± 0.3	13.98	217.8

$$l_{max} = 2\eta \frac{E_{C.M}}{V_{(R\,int)}} \left[1 - \frac{V(R_{int})}{E_{C.M}}\right]^{1/2} \qquad (9a)$$

E_{CM} is the energy in the centre of mass frame and η is the Sommerfeld parameter.

The value of grazing angle θ_{gr} is determined by using the following relation

$$\theta_{gr} = 2\tan^{-1}\left[\frac{\eta}{l_{max}}\right] \qquad (9b)$$

where l_{max} is the maximum angular momentum.

3.3 Experimental reaction cross- section from elastic data

For a given impact parameter, the incident ^{238}U ions are scattered at wide angles due to the coulomb interaction. The elastic scattering is an important process which takes place at parameter close to the sum of the radii of the colliding nuclei. The experimental differential elastic scattering cross section within angles θ_1 and θ_2 is determined as follows

$$d\sigma_{el}^{exp}\Big|_{\theta_1}^{\theta_2} = \frac{R\,A_T}{N_{av}\,\rho_t\,\phi\,a} \qquad (10)$$

where '*R*' is the number of elastic track events in a given area between angles φ_1 and φ_2 in the centre of mass frame. 'ϕ' is the fluence of incident beam.

The value of Rutherford scattering cross section σ_{Ruth} for a specific angular bin θ_2-θ_1 due to the Coulomb scattering is calculated using the expression:

$$d\sigma_{Ruth}\Big|_{\theta_1}^{\theta_2} = \pi\eta^2\lambda^2\left(\text{cosec}^2\frac{\theta_2}{2} - \text{cosec}^2\frac{\theta_1}{2}\right) \qquad (11)$$

where the Sommerfeld parameter $\eta = \mu Z_1 Z_2 e^2/\hbar^2 k$

κ is the wave number = $(1/\hbar)[2\mu E_{cm}]^{1/2}$ and $\mu = \frac{A_P A_T}{A_P + A_T}$ is the reduced mass, $E_{cm} = \varepsilon\mu$, is the centre of mass energy and ε is the energy per nucleon of the projectile.

3.4 Coulomb scattering and Fresnel model

The usual angular distribution of the elastically scattered heavy ions from a target due to the Rutherford scattering process differs in the presence of very strong Coulomb field. In such a case the trajectories of the scattered projectiles are bent at larger angles. It appears that if the incident beam is being originated from a point at a finite distance from the target, rather than from a source at infinite distance. That is why the diffraction pattern is considered to be similar to the Fresnel

diffraction, instead of Fraunhofer diffraction. Therefore, the mathematical procedure adopted is similar to that which is used to describe the scattering of light from a circular disc. The diffraction is described by the following model, for the elastic scattering cross section [11,18].

$$\frac{d\sigma_{el}^{exp}}{d\sigma_{Ruth}} = \frac{1}{2}\left\{\left[\frac{1}{2}+C(y)\right]^2+\left[\frac{1}{2}+S(y)\right]^2\right\} \quad (12)$$

where *C(y)* and *S(y)* are the real and imaginary parts of the Fresnel integrals, respectively and are defined as

$$C(y)=\int_0^y dt\cos\left[\pi t^2/2\right] \quad S(y)=\int_0^y dt\sin\left[\pi t^2/2\right] \quad (13)$$

with the argument *'y'* given by:

$$y = \frac{2\left(l_{gr}+\frac{1}{2}\right)}{\pi(\sin\theta_{gr})}\sin\frac{1}{2}(\theta-\theta_{gr}) \quad (14)$$

The Sommerfeld parameter $\eta = Z_1Z_2e^2/\hbar v$, where Z_1e, Z_2e, A_p, v and E_{lab} denote the charge numbers of the projectile and target, the mass number of the projectile, the relative velocity and bombarding energy measured in MeV, respectively.

In Eqn. 12 the ratio $(d\sigma_e/d\sigma_R)$ is the experimental elastic scattering cross section at scattering angle θ, and the Rutherford value. For pure Rutherford scattering, $l = l_{max} = l_{gr}$, l_{gr} is the grazing angular momentum and θ_{gr} is the grazing angle (when the impact parameter is just close to the sum of the radii of interacting ions). The parameters of Fresnel model are defined in terms of the quarter-point angle $\theta_{1/4}$, at the maximum impact parameter for which a nuclear reaction can occur and characterize the maximum angular momentum l_{max}, and interaction radius R_{int} for a reaction.

In this model the maximum angular momentum l_{max} for a particle interacting with the target is given by

$$l_{max} = \eta\cot\tfrac{1}{2}(\theta_{1/4}) \quad (15)$$

and $$\eta = \frac{Z_1Z_2e^2}{\hbar v} \quad (15a)$$

Z_1 and Z_2 are the charges of the target and of the projectile.

At $\theta = \theta_{gr}$, the ratio of cross sections falls to one fourth of its central value, θ_{gr} is also called quarter point angle $\theta_{1/4}$. In the strong interaction model with sharp nuclear boundaries, the relation between the total reaction cross section and quarter point angle is

$$\sigma_{el}^{exp} = \pi\lambda^2\eta^2\cot^2\left(\frac{\theta_{1/4}}{2}\right) \quad (15b)$$

The radius of interaction can also be determined by the experimental quarter-point angle

$$R_{int} = \eta\lambda\left[1+\mathrm{cosec}\left(\frac{\theta_{1/4}}{2}\right)\right] \quad (16)$$

where η is the Sommerfeld parameter, $\lambda = 1/\kappa$ is the reduced wavelength of projectile in the relative motion and κ is the projectile wave number.

Strong absorption models are developed to describe low energy reactions. In this framework the total reaction cross section is simply calculated assuming that a reaction takes place for a substantially small impact parameter between the interacting nuclei. The total reaction cross section can be expressed in terms of transmission coefficients T*(l)* through a one dimensional potential barrier calculated separately for each impact parameter or angular momentum *(l)*. It follows that

$$\sigma_R = \pi\lambda^2\sum_{l=0}^{\infty}(2l+1)T(l) \quad (17)$$

With the sharp cut-off approximation { T*(l)* = *1* for $l < l_{max}$, otherwise, T*(l)* = *0*. In a sharp cutoff model the nuclear reaction cross section, σ_R, is related to l_{max} by the expression

$$\sigma_R = \pi\lambda^2(l_{max}+1)^2 = \pi R_{int}^2\left[1-\left(\frac{V_C}{E_{CM}}\right)\right] \quad (18)$$

The model is valid for the cases where

$l_{max} >> 1$ and $l_{max} \sin \theta_{1/4} \geq 1$

R^2_{int} is strong absorption radius and V_C is the l dependent potential barrier height. From this relation one sees that the total reaction cross section saturates with increasing beam energy.

In order to estimate the quarter point angle, the elastic binary track events were separated from the total set of two-prong track events using the criterion based on the angular distribution shown in Fig. 3.

The particles scattered at nearly grazing angles appear to originate from a virtual source point at a finite distance from the target. The angular distribution in elastic scattering behaves like that of Fresnel diffraction in optics. Therefore, an analytical expression for the angular distribution in elastic scattering can be obtained using Fresnel scattering model [18]. Blair [11] has correlated the quarter-point angle $\theta_{1/4}$ with the reaction parameters, radius of interaction R_{int}, and experimental reaction cross-section (σ_{el}^{exp}). At grazing angle, the ratio of the experimental reaction cross-section (σ_{el}^{exp}) to the Rutherford cross-section ($\sigma_{Ruth.}$) falls to 1/4 and the scattering angle is called quarter-point angle ($\theta_{1/4}$). The ratio of the reaction cross-sections has been plotted as a function of scattering angle in the centre-of-mass frame and is shown in Fig. 4. The quarter-point angle ($\theta_{1/4}$) extracted from the graph is $(26.3\pm0.3)^0$. The error in the quarter-point angle is due to deviation in the sharp resolution in the angular separation of elastically scattered track events from the inelastic scattered track events. The difficulty of separation of elastic and inelastic track events arises near the angle corresponding to a grazing collision. The data at angles near the quarter-point angle ($\theta_{1/4}$) where the ration ($\sigma_{el}/\sigma_{Ruth}$) = 0.25, the number of transfer track events in the region of peak is approximately equal to the number of elastic track events.

The values in the pattern of both regions in Fig. 4 change gradually due to the increasing strength of the Coulomb interaction. The Coulomb amplitude dominates the forward scattering and the angular distribution may be divided into two regions (illuminated) $\theta < \theta_c$ and $\theta > \theta_c$ (shadow) separated by the critical angle θ_c. In the limit of strong Coulomb interaction, the cross section ratio $\sigma_{el}^{exp}/\sigma_{Ruth}$ is characterized by the features: Fresnel-type oscillation in the Coulomb region $\theta < \theta_c$, in particular a pronounced rise of σ_{exp} above the Rutherford cross section, the quarter-point property [11] ratio $\sigma_{el}^{exp}/\sigma_{Ruth} \sim 1/4$ at $\theta = \theta_c$ and a smooth decrease of $\sigma_{el}^{exp}/\sigma_{Ruth}$ in the shadow region $\theta > \theta_c$.

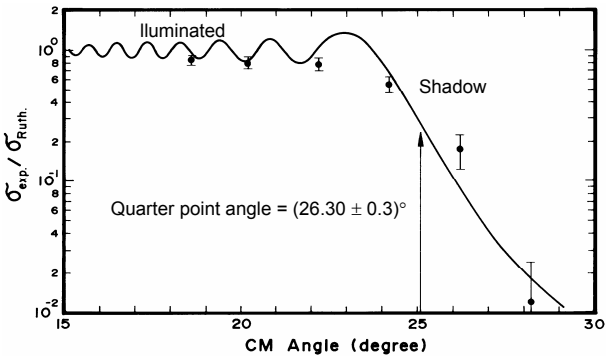

Figure 4 Normalized cross-section as function of the scattering angle in the centre-of-mass frame for the reaction (14.0 MeV/u) ^{238}U +V, using mica track detectors. The solid line shows a one parameter fit based on the absorption model. The error in the quarter-point angle is due to deviation in the sharp resolution in the angular separation of elastically scattered track events from the inelastic scattered track events.

4. Conclusions

To conclude, the interaction of (14.0 MeV/u) ^{238}U incident on a Vanadium target has been studied using mica track detectors. The elastic track events have been separated from the total number of binary track events using angular correlation criterion. The elastic data was used to determine the quarter-point angle and the reaction cross-section was calculated using the quarter-point angle $\theta_{1/4}$. The number of two-prong inelastic track events and multi-prong track events have been used to calculate the total and partial reaction cross-sections. The experimental reaction cross-sections determined from two methods (using quarter-point angle and inelastic track events) are compared with a calculation using a sharp cut-off model; measured and computed reaction cross-sections are in agreement. Due to the mixture of the quasi elastic track events in to the elastic track events, which are formed in very weakly damped reactions with binary track events, they cannot be distinguished from the elastic track events, a small

portion of the total reaction cross section goes undistinguished into the elastic channel. So the reaction cross sections obtained experimentally is measured in the lower limits of data. Different reaction parameters, in particular the radius of interaction has been derived for the heavy ions reaction studied in this work.

Acknowledgement

We are thankful to GSI, Germany for the provision of exposure facility. We also acknowledge the help of Mr. Bashir Ahmad Shad for experimental work.

References

[1] Z.C. Li, A.M. Stefanini, D.R. Napoli, G. Montagnoli, L. Corradi, C. Signorini, F. Soramel, S. Beghini and F. Scarlassara, Z. Phys **A338** (1991) 171.

[2] G. R. Satchler, Phys.Lett. **55B** (1975) 167; Phys. Rep.**199** (1991)147.

[3] P.A. Gottschalk. P. Vater, H.J. Becker, R. Brandt, G. Grawert, G. Fiedler, R. Haag and T. Rautenberg, Phys. Rev. Lett. **42** (1979) 359.

[4] M. Lefort, A. Gobbi and W. Norenberg, Heavy ion collisions, Vol. 2, Ed. R. Bock, North Holland Amsterdam (1982)

[5] M. Zamani, J. Ralarosy and M. Debeauvais; Nucl. Tracks **12** (1986) 321.

[6] P.A. Gottschalk, G. Grawert, P.Vater and R. Brandt, Phys. Rev.**C27** (1983) 2307.

[7] H.A. Khan, I.E. Qureshi, W. Westmeier, R. Brandt and P.A. Gottschalk, Phys. Rev. **C32** (1985) 1551.

[8] H.J. Wollersheim, W.W. Wilcke, J.R. Birkelund, J.R. Huizenga, W.U. Schröder, H. Freiesleben and D. Hilscher, Phys. Rev. **C24** (1981) 2114.

[9] W.U. Schröder, J.R. Birkelund, J.R. Huizenga, K.L. Wolf, J.P. Unik and V.E. Viola Jr., Phys. Rev. **C36** (1976) 514.

[10] W.W. Wilcke, J.R. Birkelund, A.D. Hoover, J.R. Huizenga, W.U. Schröder, V.E. Viola Jr, K.L. Wolf and A.C. Mignerey; Phys. Rev. **C22** (1980) 128.

[11] J.S. Blair, Phy. Rev. **95** (1954) 1218,: Phys. Rev. **108** (1957) 827.

[12] R.L. Fleisher, P.B. Price and R.M. Walker, Nuclear Tracks in Solids, University of California Press, Berkeley, USA (1975).

[13] S.A. Durrani, Radiat. Meas. **34**, Nos. 1-6 (2001) 5.

[14] S.A. Durrani and K.K. Bull, Solid State Nuclear Track Detection: Principles Methods and Applications. Pergamon Press Oxford (1989).

[15] M. Debeauvais, J. Ralarosy, J.C. Adloff, M. Zamani, F. Fernandez, S. Savovic and S. Jokic; Nucl. Tracks Radiat. Meas. **22** (1993) 571.

[16] B.G. Cartwright, E.K. Shirk and P.B.Price, Nucl. Instrum. & Meth.**153** (1978) 457.

[17] T. Tanabe, R. Bock, M. Dakowski, A. Gobbi, H. Sann, H. Stelzer, U. Lynen, A.Olmi and D. Pelte, Nucl. Phys. **A342** (1980) 194.

[18] W.E. Frahn, Nucl. Phys. **A302** (1978) 267; Phys. Rev. Lett. **26** (1971) 568, W.E. Frahn and R.H. Venter, Ann. Phys.(N.Y) **24** (1963) 243.

[19] J.J. Baloch, E.U. Khan, M.S. Zafar, I.E. Qureshi and H.A. Khan. Nucl. Instrum & Meth.**111** (1996) 91.

[20] E.U. Khan, M.I. Shahzad, F.N. Khattak, J.J. Baloch, I.E. Qureshi and H.A. Khan, The Nucleus **35**, Nos. 3-4(1998) 139.